IOP Conf. Series: Materials Science and Engineering **370** (2018) 012016 doi:10.1088/1757-899X/370/1/012016

Microvane in controlling noise in open cavity flow

M Z M Aliashak, M. R. Saad[1], A.T. Latif, A. Che Idris and M. R. A. Rahman

Department of Mechanical Engineering, Faculty of Engineering, Universiti Pertahanan Nasional Malaysia, Kem Perdana Sungai Besi, Kuala Lumpur 57000, Malaysia

[1]rashdan@upnm.edu.my

Abstract.The cavity can be commonly found in aircraft and they are used to store weapons, cargo and also landing gear. Despite the importance of cavity, they can cause vibrations and noise that can disturb the aircraft performance. In order to overcome these problems, the microvane had been studied in controlling noise on open cavity flow. The investigation was carried out at a flow speed of 64.97 meters per second with Reynolds number of 4.3×10^6 per meter on cavity with length over depth ratio of 5. The study tested two configurations of microvane which are counter-rotating and co-rotating orientation. The results show that counter-rotating microvane performed better than co-rotating microvane to suppress cavity noise. The use of counter-rotating microvane managed to reduce the sound pressure level throughout the cavity by 3 % with the highest reduction of 24 decibels. However, the co-rotating microvane cause overall increase of sound pressure level by 0.3 % with the highest reduction of 7 decibels.

1. Introduction

Nowadays, modern higher performance aircraft serve as a carriage for cargo components that are placed inside the cavities embedded in the fuselage. For modern tactical fighter aircraft, the weapons such as missiles, air-to-ground bombs and guns are stored inside the bay. Due to the importance of cavity, it has been a subject of interest in the past and also recent years.

There are three types of cavity flow which are open, transitional and closed [1]. The authors also described the boundaries at which each type occur at supersonic flow. For open cavity flow, it usually occurs at cavities with maximum length over depth *L/D* ratio less than 10. Meanwhile, closed cavity flow occurs at cavity starting from *L/D* ratio of 13 and transitional cavity flow can occur between closed and open flow cavity at *L/D* ratio from 10 to 13.

Even though the presence of cavities are common in an aircraft such as weapon bays [2-4] and landing gear [5], flow over cavity can have detrimental effects on the aircraft performance. For example, flow inside the open cavity is highly unstable and cause noise and vibrations that can lead to fatigue [6-9]. Rowley [8] and Izawa [9] stated that optical distortion and separation problems can occur inside weapon bay in a high-speed flow. Meanwhile, the flow in the closed cavity can increase drag and more susceptible to pitching up moments due to the adverse pressure gradient [1].

In order to overcome the disadvantages of cavity flow, there are two types of flow control method that can be used which are active and passive flow control. According to Jansen [10], active flow control involves additional of external energy added into the system especially into flow separation

region to overcome the problems. Among the active flow control devices that have been studied are jets [11, 12-14], pulsed energy deposition [15, 16] and oscillating fences [17]. Nonetheless, this technique is expensive and complicated in design and will not be discussed further in this paper.

Passive flow control is a method that does not require additional energy to control the cavity flow separation. The passive flow control is usually rigid geometric structure was placed at the incoming airflow and then interrupts the airflow without adding additional energy to the system [18]. In addition, this flow control technique is inexpensive and simple in design. The examples of passive flow control devices included static fences [17], spoiler [8, 14] and transverse rod [14, 19]. The purposes of passive control devices are to deflect or thicken the shear layer over the cavity to deduce its interaction with the cavity trailing edge [5, 18, 20]. Furthermore, Rowley et al [19] stated that as the amount of impingement of the shear layer, the amplitude of the resonant acoustic feedback mechanism could be reduced.

Even though there are a lot of research regarding passive control devices, they are only efficient in certain flow conditions and can cause an increase in drag. In order to overcome this issue, the use of micro vortex generator (MVG) had been proposed. MVG is a device that has height is only a fraction of a boundary layer height, δ [21]. Research conducted by Lin [22] recorded that vane shaped MVG or microvane is the best in preventing flow separation where the flow separation can be delayed up to 30 %. Furthermore, microvane also eliminate shock induced separation by producing vortices that have higher energy and much further apart that facilitate the energising of the boundary layer [23].

There are two orientations of microvane that can be commonly found which are co-rotating and counter-rotating [22, 24]. Co-rotating microvane consist of VG's arranged parallel to each other with a respective angle such as 30^{o}, 45^{o} or 60^{o}.Meanwhile, the arrangement of counter-rotating microvane needs two couples of VGs. The first VGs and third VGs have the same angle while the second VGs and fourth VGs have the same angle but in opposite way [24].

The microvane had been used in many applications such as aerofoil, fuselage and also to control flow in aircraft engine inlet system [21]. Despite the wide use of microvane in different aircraft component, there are still not many research regarding the use of microvane to control cavity flow. Therefore, this research will focus on the capabilities of microvane to control noise on closed cavity flow.

2. Methodology

The methodology of this research can be divided into several parts. The following are the details of the steps taken in conducting this research.

2.1. Design of the cavity model

SOLIDWORKS 2015 was used to model the cavity for the flow simulation. The model was designed with a curve ramp and slot where the VG will be placed. The cavity model had an *L/D* ratio of 5 with the length set 25 cm and depth of 5 cm. There are 10 points that had been marked on the cavity floor that were used for pressure measurement. Details on the dimensions of the model is shown in Figure 1.

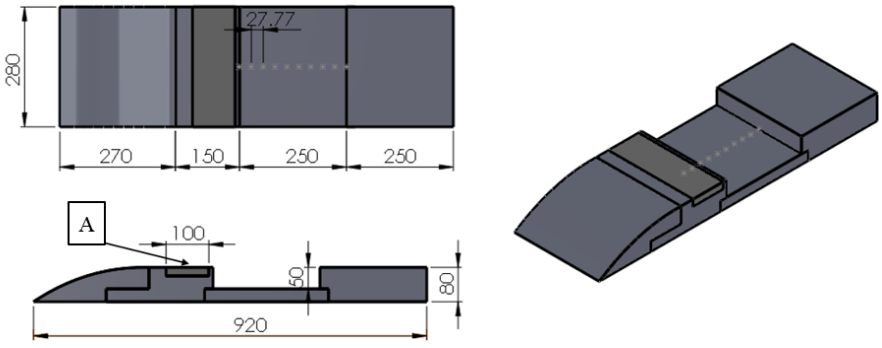

Figure 1. Dimensions of the cavity model.

2.2. Details of computation

The computational domain used was taken from [25] is shown in Figure2 and all of the solid surfaces were imposed with the no-slip condition. For all of the cases, the flow speed used was 64.97 m/s and the Reynolds number based on the cavity length was 4.3×10^6/m. The ambient pressure and temperature were set to 101.325 kpa and 20 ^oC. The model for computation was SOLIDWORKS turbulence model that was based on modified k-ε turbulence model with damping functions proposed by Lam & Bremhorst [26] where the intensity used was 0.1 % with a length of 0.0001 m. The global meshing was done using automatic settings with the highest resolution, 8 and level 4 refinement. Furthermore, the local initial mesh was also applied on all of the model top surface and inside the cavity with same resolution and level of refinement. Figure 3 and Figure 4 shows the details of the global mesh and local initial mesh where each level of meshing was labelled with letter A for coarse, B for medium and C for fine. The meshing for the simulation was set to adaptive where the size of the cell will automatically refine on the critical areas of the flow during calculation.

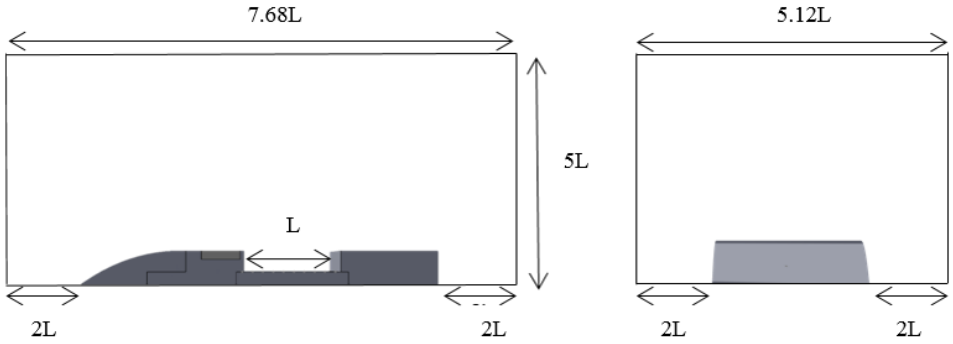

Figure 2. Size of the computational domain.

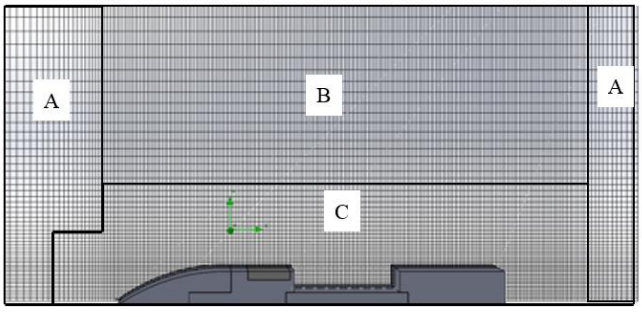

Figure 3. Simulation global mesh.

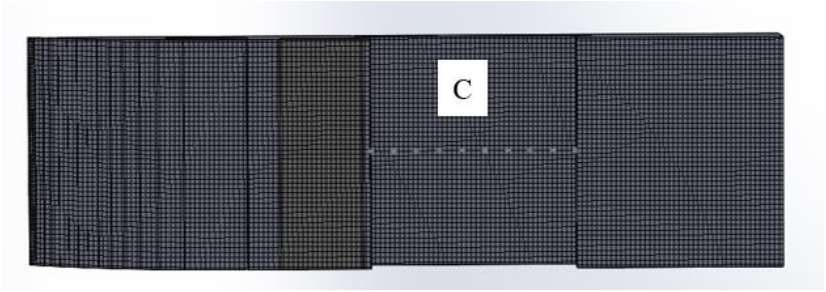

Figure 4. Simulation local initial mesh.

2.3. Microvanes parameters

The simulations were done in both counter-rotating and co-rotating microvane. Before the microvanes were tested, simulation of the clean cavity was done to determine the boundary layer thickness, δ that

was used to design the microvane. Figure 5 shows the design of microvanes and the details of the microvane dimensions are shown in Table 1.

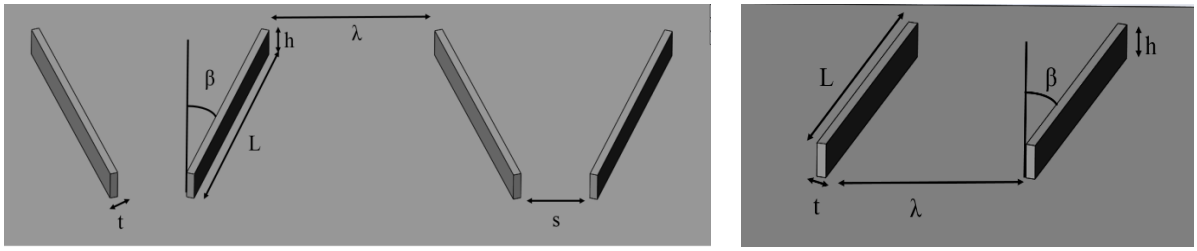

(a) (b)

Figure 5. Orientation of microvanes (a) counter-rotating (b) co-rotating.

Table 1. Dimensions of microvanes.

	h	β	t (mm)	d (mm)	L	λ	s
Counter-rotating	0.4δ	18^o	0.8	20	9h	6h	2.5h
Co-rotating	0.4 δ	18^o	0.8	20	9h	6h	-

In Table 1, the following letters h, β, t and L represents the height, angle, thickness and the microvane length. In addition, λ, s and d represent the distance between microvane, the spacing between counter-rotating microvane and also the location of microvane away from the leading edge. Details of the microvane position are shown with letter A in Figure 1.

2.4. Measurement of sound pressure level

The sound pressure level (SPL) had been chosen to quantify the ability of the microvane to suppress noise inside an open cavity. The value was computed along the cavity floor for all cases. 10 static pressure measurement along the cavity flow were taken by using the point goals function in SOLIDWORKS. Then, the pressure measurement was used to calculate the SPL using Formula 1 [27].

$$SPL\ (dB) = 20\ \log_{10}(\frac{P}{p_{ref}}) \quad (1)$$

The value of p is the pressure measured at a pressure point in Pascal and p_{ref} is the international standard for minimum audible sound 2×10^{-5} Pa.

3. Results and discussion

3.1. Validation of simulation

Validation of the flow simulation was conducted by replicating the analysis conducted by Lawson & Barakos [25] using SOLIDWORKS 2015 flow simulation software. The paper was chosen due to the similarity in the type of cavity used, the parameter used to quantify the cavity noise suppression. The cavity model was positioned at zero yaw and pitch angle with the Mach number of the flow set to 0.85. The cavity had a length of 20 inches and depth of 4 inches with the *L/D* ratio of 5. The simulation was conducted without using any flow control devices and the pressure was measured at ten points along the floor of the cavity.The data obtained from the validation were collected and compared with the experimental data. The pressure readings obtained were used to calculate the SPL. Figure6 shows the comparison between the SPL on cavity floor from the simulation and experiment Lawson & Barakos [25].

Figure 6 shows that the magnitude of the SPL was different for four points along the cavity between x/L = 20 % to x/L = 60 %. This might be caused by the turbulence model used by SOLIDWORKS were different compared to the one used by Lawson & Barakos [25].Even though, the simulation shows some discrepancies, the overall margin of error between the simulation and experiment were within 3% which is in line with the research conducted by the authors [25].

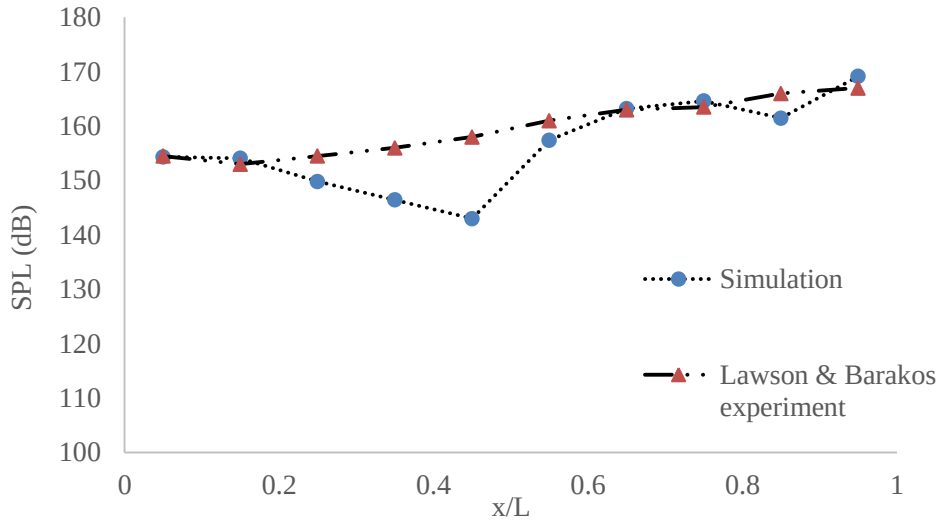

Figure 6. Comparison of SPL distribution across cavity floor.

Furthermore, the validation was also done qualitatively on the model of the cavity baseline. The streamline plot for the simulation was compared the description of the open cavity from Lada & Kontis [11]. Research from the authors was used as a comparison due to the same type of cavity and also similar flow speed. The comparison between the cavity flows is shown in Figure 7.

From Figure 7, the simulation shows similarities with Lada & Kontis [11] where there is huge recirculation of flow inside the cavity. Even though the experiment conducted by the authors have slightly higher flow speed at 100 m/s and lower *L/D* ratio of 2 both experiments shows that there is huge recirculation of flow inside the cavity. The simulation also shows that there was a high-pressure region at the trailing edge of the cavity as described in by the authors [11]. This indicates that the simulation conducted manage to simulate the flow inside an open cavity accurately. From the quantitative and qualitative analysis, it was concluded that the simulation conducted in SOLIDWORKS flow simulation was valid

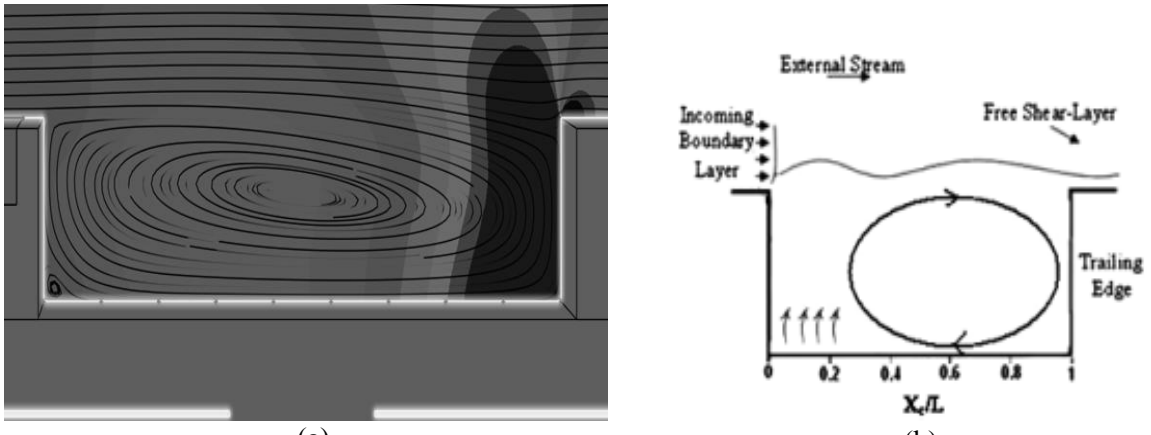

(a) (b)

Figure 7. Comparison between open cavity flow (a) simulation (b) Lada & Kontis [11].

3.2. Baseline cavity without microvane

Simulation with the baseline was conducted to determine the boundary layer thickness. It was found that the region where the microvane was located had a boundary layer ranging from 5 mm to 7.5 mm. Meanwhile, the SPL distribution of clean cavity is shown in Figure 8. From the figure, it can be seen that the distribution of the SPL gradually increasing up to x/L = 0.44 where the SPL started to drop until it reaches the lowest point at x/L = 0.67 with 125 dB. After that, the reading of the SPL increased rapidly until x/L = 1 where the highest reading recorded with 154 dB.

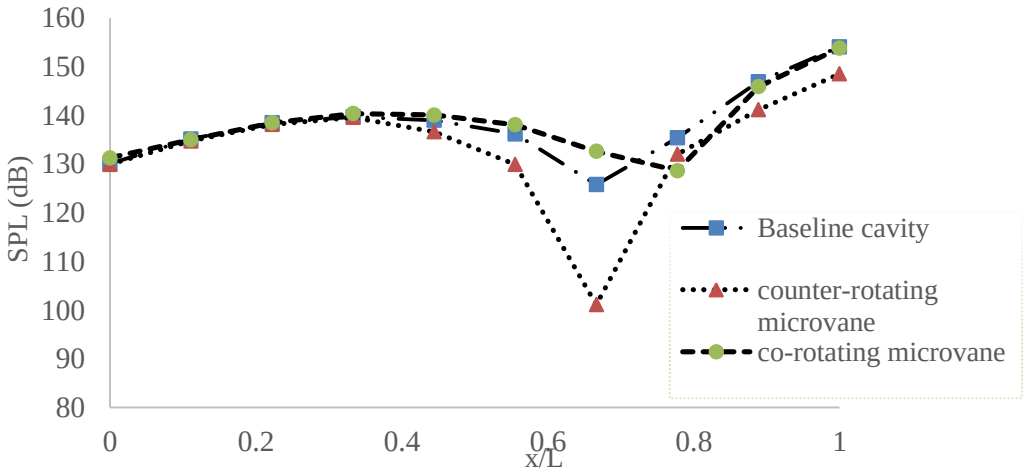

Figure 8. SPL distribution across cavity floor for all cases tested.

3.3. Effect of counter-rotating microvane on cavity flow

Figure 8 also shows the comparison between the cavity SPL with and without the counter-rotating microvane. All of the points inside the cavity with counter-rotating microvane shows a drop of SPL. A significant drop of SPL can be seen from x/L = 0.55 until x/L = 1 where the highest drop can be seen at x/L = 0.67 where the SPL was reduced by 24 dB. On the overall, the SPL value drops by 3.7 % compared to the clean cavity. The reduction of SPL occurs due to the counter-rotating vortices generated by the counter-rotating microvane that can be seen in Figure 9. Figure 10 suggested that the vortices generated by the counter-rotating microvane reduce the impingement on the trailing wall of the cavity which was marked with the letter A. The counter-rotating microvane also caused another recirculation inside the cavity that was shown in Figure 11 and was marked with the letter B. This increase of circulation reduced the pressure throughout the cavity which in turn causes reduction in the SPL.

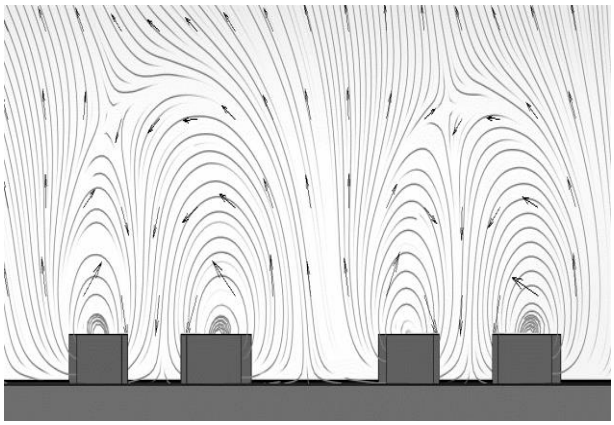

Figure 9. Vortices generated by counter-rotating microvane.

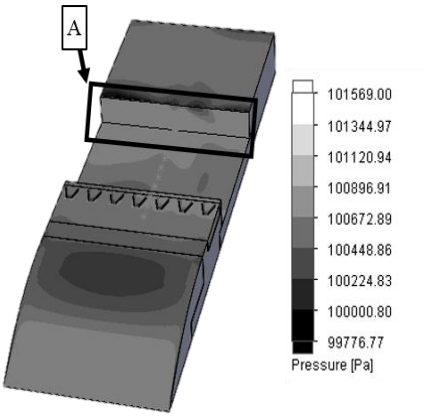

Figure 10. Pressure surface plot for counter-rotating microvane.

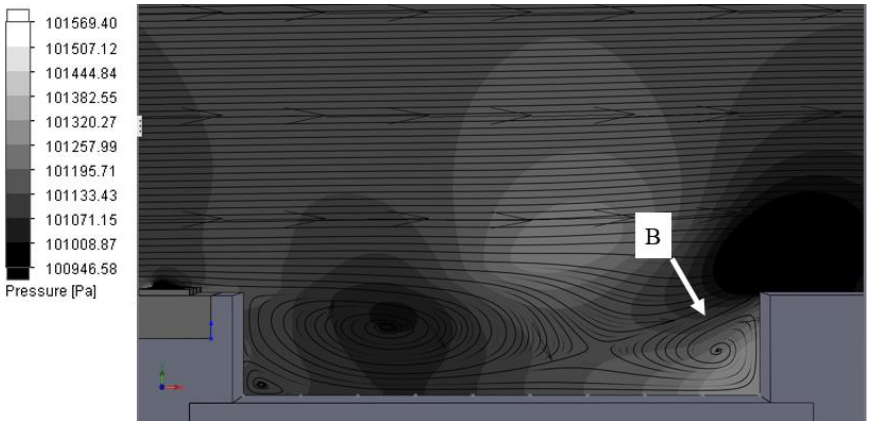

Figure 11. Pressure contour plot for counter-rotating microvane.

3.4. Effect of co-rotating microvane on cavity flow

The co-rotating microvane does not significantly improve the SPL of the cavity. From Figure 8, the region where reduction of SPL can be seen from x/L = 0.78 until x/L = 1 with the highest decrease of SPL occurred at x/L = 0.78 where it was reduced by 7 dB. However, the SPL at x/L = 0 and at x/L = 0.33 until x/L = 0.67 were higher than clean cavity. On overall, the use of co-rotating microvanes increases the cavity SPL by 0.3 %. Figure 12 shows that co-rotating microvane also generated vortices similar to counter-rotating microvane but in co-rotating direction. However, Figure 13 shows that the impingement of the shear layer on the cavity trailing wall was much intense than counter-rotating microvane which was marked with the letter A. Figure 14 also shows that the flow condition inside the cavity does not differ from the baseline. Therefore, it was assumed that the vortices generated by co-rotating microvane were not effective in altering the flow and controlling the noise inside the cavity.

3.5. Comparison between counter-rotating and co-rotating microvane on cavity flow

The counter-rotating performed better than co-rotating microvane in reducing the SPL. The SPL recorded for the cavity with counter-rotating microvane were lower on every point except the eight point which located on x/L = 0.78. In total, the counter-rotating microvane performed better by 3.8 % in reducing the cavity SPL. This shows that the vortices generated by counter-rotating microvane are more effective at energising shear layer for a cavity with *L/D* ratio of 5.

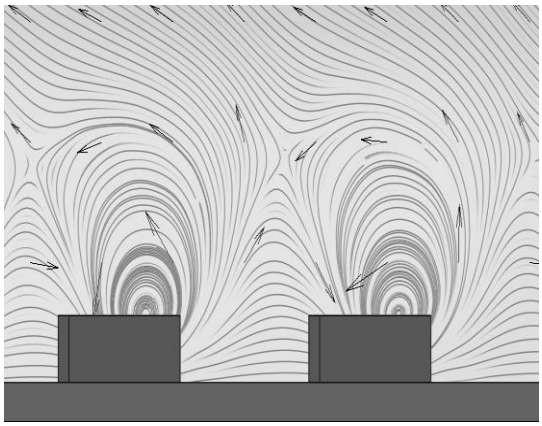

Figure 12. Vortices generated by co-rotating microvane.

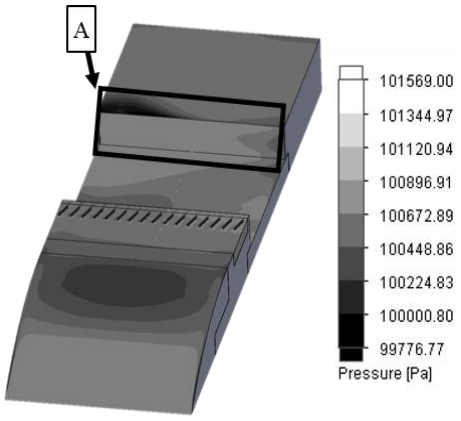

Figure 13. Pressure surface plot for co-rotating microvane.

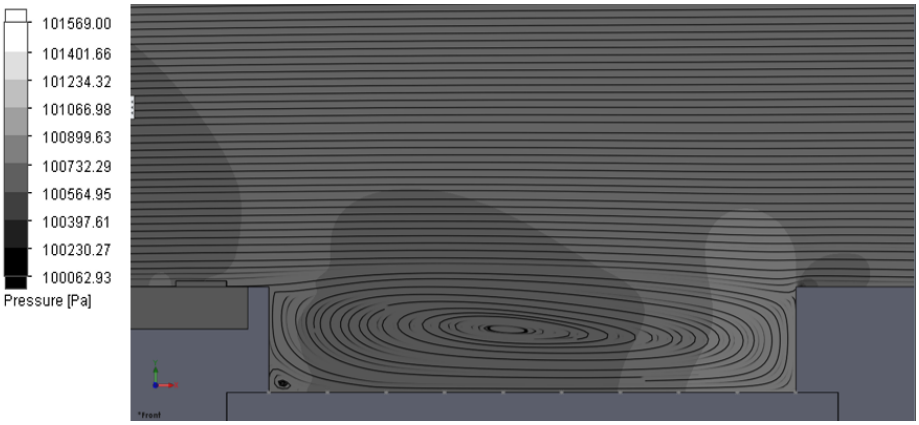

Figure 14. Pressure contour plot for co-rotating microvane.

4. Conclusions

In this study, the effects of microvane to control cavity flow with *L/D* ratio of 5 at Reynolds number of 4.3×10^6 /m had been conducted. The results show that counter-rotating microvane performed better than co-rotating microvane in controlling cavity flow. Counter-rotating microvane generated vortices that have the capability to reduce the SPL throughout the cavity. For co-rotating microvane, the SPL increase until x/L = 0.67 and started to decrease until the trailing edge of the cavity. The results also indicate that vortices generated by co-rotating microvane do not have a significant impact on altering the flow inside the cavity. This shows that the counter-rotating microvane have a high potential to be used as an alternative to other passive control devices to suppress noise in an open cavity.

References

[1] Maureen B, Tracy, and Plentovich EB. Cavity unsteady-pressure measurements at subsonic and transonic speeds, NASA TP-3669,1997.
[2] Shaw, L., Clark, R., and Talmadge, D., F-111 Generic Weapons Bay Acoustic Environment, *Journal of Aircraft*, **Vol. 25**, No. 2, 1988, pp. 147–153.
[3] Cattafesta, III L, Shukla D, Garg S, Ross J. Development of an adaptive weapons-bay suppression system. *In5th AIAA/CEAS Aeroacoustics Conference and Exhibit* 1999 (p. 1901).
[4] Bower WW, Kibens V, Cary AW, Alvi FS, Raman G, Annaswamy A, Malmuth NM. High-frequency excitation active flow control for high-speed weapon release (HIFEX). AIAA paper. 2004 Jun;2513:2004.
[5] Mitchell, Douglas. Control of High-Speed Cavity Flow Using Plasma Actuators. Diss. The Ohio State University, 2006.
[6] Tracy, Maureen B.; and Stallings, Robert L., Jr. Coupling of Acoustic Environment in Rectangular Cavity With Store Vibration Characteristics During Simulated Separation in Supersonic Flow. NASA TP-2986, 1990
[7] Shaw, L. L.; and Shimovetz, R. M. Weapons Bay Acoustic Environment. Impact of Acoustic Loads on Aircraft Structures, AGARD-CP-549, Sept. 1999
[8] C. W. Rowley. Modelling, simulation and control of cavity flow oscillations. PhD thesis, Institute of Technology Pasadena, California, 2002.
[9] S. Izawa. Active and passive control of flow past a cavity. Wind Tunnel and Experimental Fluid Dynamics Research, Tohoku University, Japan, 2011.
[10] D. P. Jansen. Passive flow separation control on an airfoil flap model the effect of cylinders and vortex generators. Master thesis, Deflt University of Technology, Netherland, 2012
[11] Lada C, Kontis K. Microjet Flow Control Effectiveness of Cavity Configurations at Low Speeds. *Journal of Aircraft*. 2014 Sep 24.

[12] Vakili AD, Gauthier C. Control of cavity flow by upstream mass-injection. *Journal of Aircraft*. 1994 Jan 2;31(1):169-74.
[13] Bueno P, Unalmis O, Clemens N, Dolling D. The effects of upstream mass injection on a Mach 2 Cavity Flow. *In40th AIAA Aerospace Sciences Meeting & Exhibit 2002* (p. 663).
[14] Ukeiley LS, Ponton MK, Seiner JM, Jansen B. Suppression of Pressure loads in resonating cavities through blowing. AIAA Paper. 2003 Jan;181:2003.
[15] Lazar ES, Elliott G, Glumac N. Control of the shear layer above a supersonic cavity using energy deposition. Diss. University of Illinois at Urbana-Champaign, 2008.
[16] Adelgren RG, Elliott GS, Crawford JB, Carter CD, Donbar JM, Grosjean DF. Axisymmetric jet shear-layer excitation by laser energy and electric arc discharges. *AIAA journal*. 2005 Apr 1;43(4):776-91.
[17] Sarno RL, Franke ME. Suppression of flow-induced pressure oscillations in cavities. *Journal of Aircraft*. 1994 Jan 2;31(1):90-6.
[18] Danilov PV, Quackenbush TR. Flow Driven Oscillating Vortex Generators for Control of Cavity Resonance. *In49th AIAA Aerospace Sciences Meeting including the New Horizons Forum and Aerospace Exposition* 2011 (p. 1219).
[19] C. W. Rowley, V. Juttijudata and D. R. Willicas. Cavity for control simulation and experiments. AIAA Paper 2005-0292, 2005.
[20] Smith B, Welterlen T, Maines B, Shaw L, Stanek M, Grove J. Weapons bay acoustic suppression from rod spoilers. AIAA Paper. 2002 Jan 14;662:2002.
[21] Lin JC. Review of research on low-profile vortex generators to control boundary-layer separation. *Progress in Aerospace Sciences*. 2002 Jul 31;38(4):389-420.
[22] Lin J. Control of turbulent boundary-layer separation using micro-vortex generators. *In30th Fluid Dynamics Conference* 1999 (p. 3404).
[23] Holden HA, Babinsky H. Vortex generators near shock/boundary layer interactions. AIAA paper. 2004 Jan 8;1242:2004.
[24] Jansen DP. Passive Flow Separation Control on an Airfoil-Flap Model. Deft University. 2012 Aug.
[25] Lawson SJ, Barakos GN. Assessment of passive flow control for transonic cavity flow using detached-eddy simulation. *Journal of Aircraft*. 2009 May 1;46(3):1009.
[26] Lam, C K G and Bremhorst, K A Modified Form of Model for Predicting Wall Turbulence. *ASME Journal of Fluids Engineering*, 1981, **Vol. 103**, pp. 456-460
[27] Ruth F Weiner and R Matthews*Environmental Engineering fourth edition* Butterworth Heineman 2003 p 428

Acknowledgements
The authors would like to thank the Ministry of Education Malaysia for the financial support under the RAGS (RAGS/1/2014/TK09/UPNM/1), RACE (RACE/F3/PK6/UPNM/13) and UPNM GPJP (UPNM/2015/GPJP/2/TK/09) research grant schemes. Also an appreciation to the technical staffs of the Faculty of Engineering, UniversitiPertahanan Nasional Malaysia for providing the assistances to the equipment and computing facilities.